Tuning the underwater adhesiveness of antibacterial polysaccharides complex coacervates

Perrine Galland, Muhammad Haseeb Iqbal, Damien Favier, Mélanie Legros, Pierre Schaaf, Fouzia Boulmedais, Mehdi Vahdati

Journal of Colloid and Interface Science 661 (2024) 196–206

Contents lists available at ScienceDirect

Journal of Colloid And Interface Science

journal homepage: www.elsevier.com/locate/jcis

Tuning the underwater adhesiveness of antibacterial polysaccharides complex coacervates

Perrine Galland [a,1], Muhammad Haseeb Iqbal [a,1], Damien Favier [a], Mélanie Legros [a], Pierre Schaaf [a,b,c], Fouzia Boulmedais [a,*], Mehdi Vahdati [a,*]

[a] Université de Strasbourg, CNRS, Institut Charles Sadron, UPR 22, 67200, Strasbourg, France
[b] Institut National de la Santé et de la Recherche Médicale, INSERM Unité 1121, Biomatériaux et Bioingénierie, 67000, Strasbourg, France
[c] Université de Strasbourg, Faculty of Dental Surgery, 67000, Strasbourg, France

GRAPHICAL ABSTRACT

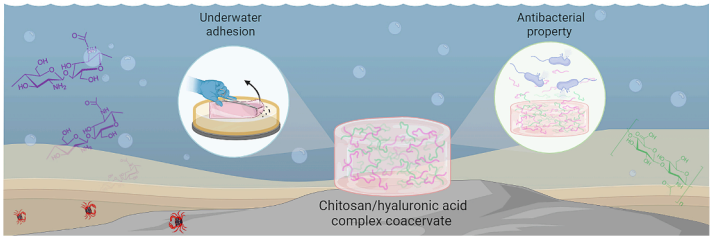

ARTICLE INFO

Keywords:
Bio-sourced polymers
Biomaterials
Physical hydrogels
Weak interactions
Electrostatic interactions
Polyelectrolytes
Soft adhesives

ABSTRACT

Hypothesis: Adjusting the water content and mechanical properties of polyelectrolyte coacervates for optimal underwater adhesion requires simultaneous control of the macromolecular design and the type and concentration of the salt used. Using synthetic or bio-inspired polymers to make coacervates often involves complicated chemistries and large variations in salt concentration. The underwater adhesiveness of simple, bio-sourced coacervates can be tuned with relatively small variations in salt concentration. Bio-sourced polymers can also impart beneficial biological activities to the final material.

Experiments: We made complex coacervates from charged chitosan (CHI) and hyaluronic acid (HA) with NaCl as the salt. Their water content and viscoelastic properties were investigated to identify the formulation with optimal underwater adhesion in physiological conditions. The coacervates were also studied in antibacterial and cytotoxicity experiments.

Findings: As predicted by linear rheology, the CHI-HA coacervates at 0.1 and 0.2 M NaCl had the highest pull-off adhesion strengths of 44.4 and 40.3 kPa in their respective supernatants. In-situ physical hardening of the 0.2 M coacervate upon a salt switch in 0.1 M NaCl resulted in a pull-off adhesion strength of 62.9 kPa. This material maintained its adhesive properties in physiological conditions. Finally, the optimal adhesive was found to be non-cytotoxic and inherently antimicrobial through a chitosan release-killing mechanism.

* Corresponding authors.
E-mail addresses: fouzia.boulmedais@ics-cnrs.unistra.fr (F. Boulmedais), mehdi.vahdati@ics-cnrs.unistra.fr (M. Vahdati).
[1] These authors contributed equally to this work.

https://doi.org/10.1016/j.jcis.2024.01.193
Received 23 September 2023; Received in revised form 22 January 2024; Accepted 26 January 2024
Available online 28 January 2024

1. Introduction

Extracted from various natural organisms, bio-sourced polymers come in a wide range of chemistries, often feature good biocompatibility, and, in some cases, have other interesting biological functions such as antibacterial activity. These polymers have thus become one of the key components of the materials toolbox for various biomedical applications such as tissue engineering, drug delivery, and tissue adhesives. Polysaccharides such as hyaluronic acid, chitosan, and alginate have been widely used in these applications.[1,2].

Current designs of tissue adhesives based on bio-sourced polymers rely on the *in-situ* crosslinking of a polymer solution. Meanwhile, reactions with the functions present on tissue surfaces allow the adhesive to chemically bond to the tissue.[3–5] Tissue adhesives offer multiple advantages over sutures and staples. These include less traumatic (minimally invasive) wound closure, protection from potential infection, promotion of wound healing, and better cosmetic results for external wounds. However, the crosslinking strategy has its limitations and inconveniences such as (i) toxicity of the crosslinking reactions (even when the polymers used are not toxic), (ii) excessive heat release (exothermic reactions), and (iii) low adhesion strengths. [6,7].

Examples of polysaccharide-based tissue adhesives prepared as described above are ubiquitous in the literature. For instance, tissue adhesives have been reported based on chemical hydrogels of chitosan (CHI) modified with a tyramine-modified polyethylene glycol [8], phloretic acid [9], hydrocaffeic acid and hydrophobic side chains [10], and gallic acid moieties [11]. Similarly, chemical hydrogels of hyaluronic acid (HA) were modified with aldehydes [12], dopamine hydrochloride [13,14], polydopamine nanoparticles [15], and phenylboronic acid [16] to obtain adhesion to wet biological tissues. The majority of these hydrogels were crosslinked under oxidative conditions using reagents like sodium periodate and hydrogen peroxide or photo-crosslinked in the presence of a photoinitiator. The wet adhesion strengths (maximum detachment force normalized by the contact area in shear or pull-off) reported in these works varied in the range of 5 to 90 kPa.

An alternative approach to chemical crosslinking is to develop materials that are, and that ideally remain, *sticky* in aqueous media as a model for the biological environment. The stickiness is either a fine-tuned inherent property of the material or is induced by an external stimulus such as pH or temperature. These underwater adhesives do not rely on specific interfacial interactions. Rather, the viscoelastic properties of the material may be tuned such that it can form intimate contact with various substrates and resist the applied stresses to dissipate large amounts of energy during debonding.[7] These materials must have (i) a storage modulus (G') well below 0.1 MPa on the time scale of bonding (1 Hz; known as the Dahlquist's criterion [17,18]) and (ii) a loss factor ($tan(\delta)$ = the ratio of the loss modulus (G'') to the storage modulus) between 0.3 and 1.0.[19–21] It must be noted that these criteria are necessary but not always sufficient for a material to exhibit the typical behavior of hydrophobic pressure-sensitive adhesives (PSAs).

Complex coacervates, formed via associative phase separation of oppositely charged polyelectrolytes in water, are water-rich soft materials with widely adjustable mechanical properties from soft gel-like solids to viscous liquids. It is important to note that changes in the mechanical properties of these materials are closely linked to changes in their composition, especially the water content.[7,22] The tunability of the mechanical properties of complex coacervates and their typically large water contents (60 – 90 wt%) make them promising candidates for biomedical purposes. These materials can also be designed as liquid-like or soft, solid-like complex coacervates that harden in physiological salt concentration in a so-called *salt switch*, as previously studied in model [23,24] and bio-inspired [25] systems. This strategy relies on the diffusion of salt out of the material (driven by higher salt concentrations in the coacervate than in the medium) and the formation of additional physical crosslinks.

As briefly introduced above, the underwater adhesive properties of complex coacervates may be predicted and tuned based on their linear viscoelastic properties. The majority of complex coacervates studied as underwater adhesives have been based on synthetic model polyelectrolytes or bioinspired polyelectrolytes with complicated chemistries. The reported underwater adhesion strength of these polyelectrolyte complex coacervates without further modifications, chemical crosslinking, and or resorting to other weak interactions is between 7 and 50 kPa. [7] We note that given the viscoelastic and thus rate-dependent nature of these materials, adhesion strength values from different reports must be compared with caution. Nonetheless, the current state of the art clearly suggests that it is possible to exploit electrostatic interactions to develop underwater adhesives with comparable performance to chemical hydrogels. Exploring widely available, non-toxic, and preferably bio-sourced polyelectrolytes seems like a reasonable next step in the development of coacervate-based underwater adhesives.

Chitosan and hyaluronic acid are linear polysaccharides bearing positively and negatively charged functional groups at mildly acidic pH, respectively (Fig. 1**A**). CHI is known to possess antibacterial activity[26] while HA plays an important role in tissue hydration, water transport, and inflammatory response after trauma [1,27]. Perry's group reported on the effect of solvent quality on the phase behavior and the rheological properties of CHI-HA complex coacervates at pH 4.5 where both polymers are fully charged.[28] The authors showed that the rheological behavior of these complex coacervates is very sensitive to small changes in salt (NaCl) and cosolvent concentrations. Interestingly, increasing the NaCl concentration from 0.3 M to 0.6 M transformed the initially soft, viscoelastic solid-like materials into highly viscoelastic liquid-like coacervates.

More recently, Kamperman's group performed a detailed investigation into the phase behavior and viscoelastic properties of CHI-HA complex coacervates at pH 4.0 and 6.0.[29] At pH 6.0, the authors found clear evidence of dynamically arrested domains due to extensive hydrogen bonding resulting from the partially protonated amine groups of CHI at this pH. The resulting materials were thus soft elastic gels with little sensitivity to salt concentration. Nonetheless, at the lower pH where CHI is almost fully charged, the dynamics of the system was controlled only by electrostatic associations and was adjustable as a function of the salt concentration. The intriguing tunability of the dynamics of this system at relatively low NaCl concentrations may be exploited to design soft adhesives adapted to physiological environments.

Non-cytotoxic, degradable, hemostatic, and antibacterial, CHI is widely used to develop materials (such as films, hydrogels, sponges, nanofibers, etc.) for biomedical applications, in particular as wound dressings.[1,30] Naturally found in the body, highly hydrated, and recognized specifically by CD44 cell receptor, HA is used to develop nanoparticles, hydrogels, or scaffold for drug delivery and tissue engineering.[1,31].

Despite multiple examples of each polymer in the development of tissue adhesives (as briefly reviewed above), no study has focused on the underwater adhesive properties of complex coacervates based on CHI and HA. This work introduces a rational design of CHI-HA complex coacervate-based underwater adhesives based on their linear viscoelastic properties. As shown in Fig. 1**B** and **C**, these materials are simply obtained by mixing and centrifuging high molecular weight polysaccharides in NaCl solution. We emphasize that the preparation involves no chemical reactions or modifications whatsoever. After the determination of the coacervates' water content, the most promising underwater adhesives are identified based on underwater rheological measurements at 37 °C. The viscoelastic properties of CHI-HA complex coacervates are studied (i) immersed in their respective supernatant, (ii) upon a salt switch, i.e. immersed in 0.1 M NaCl at pH 5.0, and (iii) immersed in phosphate-buffered saline (PBS) at 0.137 M NaCl at pH 7.4

where they experience both a salt and a pH switch. We verify our predictions by well-controlled underwater pull-off tests performed immediately after each rheological measurement. Importantly, the most performant complex coacervate is shown to be antibacterial and non-cytotoxic, making it a promising candidate for potential biomedical applications.

2. Experimental

2.1. Materials

High MW Chitosan (base form) with a deacetylation degree of 72.1 % (confirmed via ^{1}H NMR) was purchased from Sigma-Aldrich. The weight average molecular weight was measured via Size Exclusion Chromatography (*SEC*) to be 548 kg.mol^{-1} (M_w/M_n = 2.36). High molecular weight Hyaluronic Acid was purchased from Lifecore Biomedical. The weight average molecular weight measured via *SEC* was 400 kg.mol^{-1} (M_w/M_n = 2.1). The characterizations performed on the polymers is detailed in the Supporting Information. Sodium chloride (NaCl) was purchased from Fisher Chemical. 1-ethyl-3-(3-dimethylaminopropyl) carbodiimide (EDC) and *N*-hydroxysuccinimide (NHS) were purchased from Sigma Aldrich. MilliQ water was used in all experiments. pH Adjustments were done using small quantities of concentrated solutions of HCl and or NaOH.

2.2. Preparation of CHI-HA complex coacervates

Prior to sample preparation, all the glassware was washed with MilliQ water, rinsed with ethanol, and dried at 80 °C for 30 min to remove potential biological contaminations. First, stock solutions of the individual polymers and NaCl were prepared. CHI was dissolved at 1 wt % in 0.1 M HCl (pH 1) by extensive stirring for 48 h at 50 °C. The solution was then filtered against 45 μm pore-sized sterile filters (polyethersulfone (PES) membranes, SARSTEDT) and the pH was adjusted to 5 using a concentrated solution of NaOH. Changes in concentration were taken into account. HA was dissolved at 2 wt% in MilliQ water at pH 5 and filtered against 20 μm pore-sized sterile filters (polyethersulfone (PES) membranes, SARSTEDT) before use. A 3 M stock solution of NaCl at pH 5 was made and filtered against the 20 μm filters mentioned above.

All the complex coacervates were prepared at pH 5 where the charge ratio between the oppositely charged groups of the two polymers is nearly stoichiometric.[28,32] The total polymer concentration was fixed at 1.12 wt%, corresponding to a total charged group concentration of 39 mM. The complex coacervates were prepared with a slight deviation from stoichiometry in favor of the carboxylic acid groups from HA (1.1: 1.0 carboxylic acid: amine groups). At each salt concentration, the calculated amount of the stock NaCl solution was added to 5.35 mL HA under stirring. To this, 6.80 mL of CHI was added in one shot, immediately resulting in a turbid or hazy mixture (at salt concentrations where complex coacervation took place). The stirring was continued for 3 h before transferring the samples into Falcon® Tubes. After 24 h of rest, the samples were centrifuged at 9500 rpm for 30 min. All the samples were prepared in triplicates on different days and from different stock solutions to ensure reproducibility. The samples used in all the experiments are those after centrifugation, unless otherwise mentioned.

Carbodiimide cross-linked CHI-HA coacervates were obtained by incubating 35–40 mg CHI-HA coacervates in 0.2 mL of 200 mM EDC/ 50 mM sulfo-NHS solution in 150 mM NaCl at pH 5.5 for 18 h at room temperature, followed by rinsing the coacervates using 150 mM NaCl solution for 2 h.

2.3. Water content determination

The determination of the water content using Thermo Gravimetric Analysis (TGA) was performed on a thermal analysis system (TGA2, Mettler-Toledo) following a procedure detailed elsewhere.[24] Briefly, for each sample, the supernatant phase was removed carefully and between 10 and 40 mg of the complex coacervate were placed in 150 µL

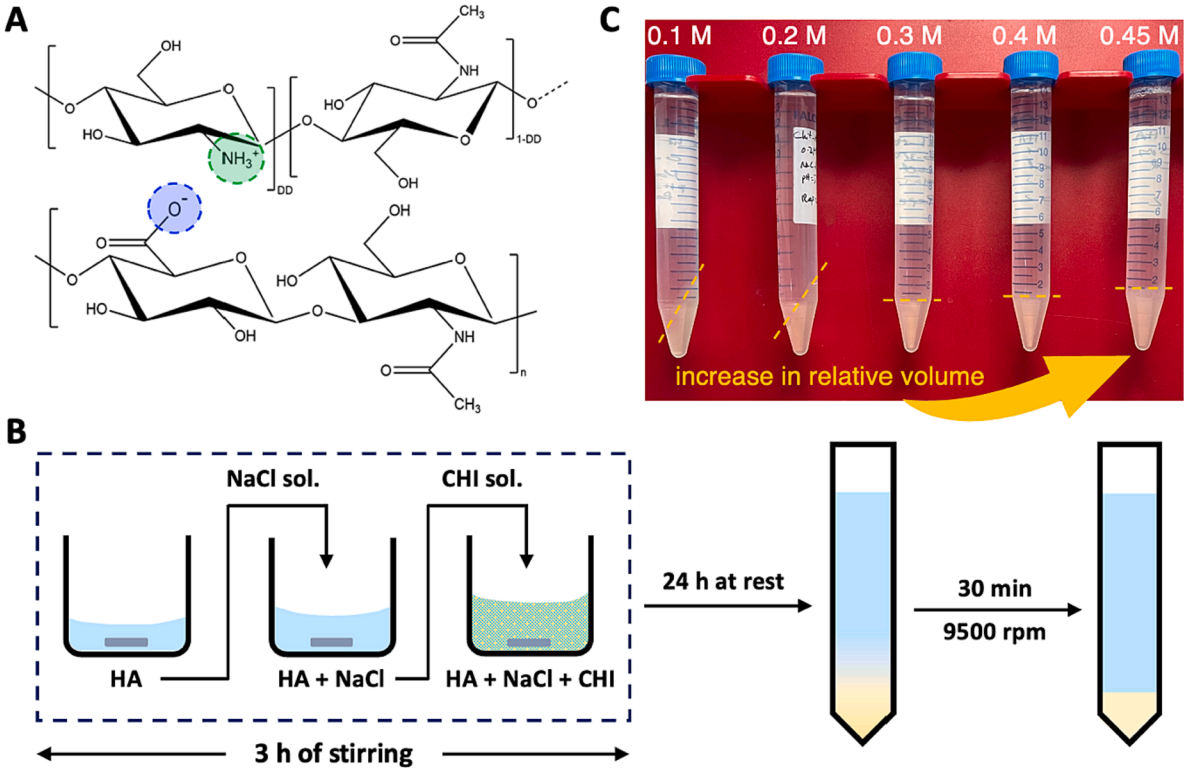

Fig. 1. (A) The chemical structure of chitosan (CHI, top) and hyaluronic acid (HA, bottom) in the charged state. (B) Schematic representation of the preparation of CHI-HA complex coacervates. (C) The CHI-HA complex coacervate samples at different NaCl concentrations prepared at pH 5.0.

Alumina crucibles. The sample was heated at 10 °C.min^{-1} up to 150 °C under air, where it was maintained for 20 min. The mass loss at the end of this procedure was taken as the content of water. We verified the occurrence of no further mass loss upon heating up to 200 °C. The reported water contents correspond to at least three measurements on independently prepared samples.

2.4. Microscopy observations

Aliquots taken 1 h after mixing the two polyelectrolytes, i.e. before resting and centrifugation, were imaged under an inverted optical microscope (Zeiss). The aliquots were placed between two glass slides separated with a spacer and observed at different magnifications.

2.5. Underwater linear rheology

Linear rheology experiments were performed on a Discovery HR-20 (TA Instruments) rheometer, equipped with a Peltier plate and a reservoir cup around the geometry. All rheological experiments were performed at 37 °C in the aqueous medium mentioned for each test. The geometry used was a sandblasted INOX flat plate with a radius of 10 mm. The medium was added after the sample was gently squeezed down to a thickness of $h_0 = 500\ \mu m$. Frequency sweeps were performed at 0.1 % strain (verified to be in the linear regime). The time sweeps to follow salt switch experiments were performed at 0.1 % strain and 10 rad.s^{-1}. In this case, the immersion medium was added 60 s after the onset of the time sweep.

2.6. Underwater pull-off tests

Underwater pull-off tests were performed on a rheometer (Discovery HR-20, TA Instruments) following a procedure described previously. [33] In this case, the pull-off tests were performed immediately after the linear rheology experiments (frequency or time sweeps), i.e. keeping the same aqueous medium and geometry at 37 °C. The initial thickness of the adhesive film was 500 μm. The flat probe was pulled off at a constant debonding velocity of 100 $\mu m.s^{-1}$, corresponding to a nominal strain rate of 0.2 s^{-1}. The pull-off force was recorded as a function of displacement. The maximum pull-off force normalized by the initial contact area, called the underwater adhesion strength, is presented as a failure criterion for the adhesives. The reported values are the average of three measurements on independently prepared and tested samples.

2.7. Antibacterial activity

Antibacterial tests were carried out employing one strain of Gram-positive bacteria, *Staphylococcus aureus* (*S. aureus*, ATCC 25923), and another strain of Gram-negative bacteria, *Escherichia coli* (*E.coli*, ATCC 25922). *S. aureus* and *E. coli* were precultured separately in aerobic conditions at 37 °C in a Mueller Hinton (MH) and Luria-Bertani (LB) broth medium (Merck, Germany), respectively, at pH 7.4. One colony from previously prepared agar plates by bacteria streaking protocol was transferred to 7 mL of MH or LB medium and incubated in an agitator overnight at 37 °C. To obtain bacteria in their mid-logarithmic phase of growth, the absorbance at 620 nm (OD_{620}) of overnight cultures was adjusted to 0.001 by diluting in RPMI (Roswell Park Memorial Institute) cell culture medium, corresponding to a final cell density of approximately 8×10^5 CFU/mL. Cultures growing in the presence of antibiotics (Tetracycline and Cefotaxime) were taken as positive control. Bacteria quantification (in colony forming unit per mL, CFU/mL) was performed after 24 h of incubation with the samples. This was determined by plating 100 µL of the supernatant, after serial dilution, on nutrient agar plates at 37 °C overnight, followed by counting the viable cell colonies (CFU/mL). 35–40 mg CHI-HA 0.2 M coacervates were placed in 96-well plates and sterilized for 20 min by UV light. 100 µL of *S. aureus* or *E. coli* inoculation ($OD_{620} = 0.001$) were added to each well and incubated at 37 °C for 24 h. The quantification of adherent bacteria on CHI-HA coacervates and tissue culture polystyrene, TCPS, (Ctrl) was performed after 24 h of incubation as follows. After the removal of the bacterial suspension, CHI-HA and TCPS were gently rinsed with PBS to remove non-adherent bacteria. Adherent bacteria were then detached in PBS using an ultrasonication step in an ultrasonic bath for 7 min. The number of living adherent bacteria was determined as previously detailed. Regarding the statistical analysis, all experiments were carried out independently in triplicate and three analyses per replication at least were performed. The significant differences in the experimental data were analyzed using the Student's *t*-test procedure.

2.8. Cell cytotoxicity test

Cytotoxicity assays were carried out by incubating CHI-HA coacervates with 0.1 mL of DMEM High Glucose supplemented with 10 % decomplemented Fetal Bovine Serum and 1 % penicillin streptomycin at 37 °C. After seeding the cells for 24 h, the extracts were removed under sterile conditions. Separately, BALB 3 T3 mouse fibroblast cells, cell passage from 17 to 19, were seeded at a density of 1×10^4 cells/mL in a supplemented medium in a sterile 96-well culture plate and incubated to confluence. After 24 h of incubation, the medium was replaced with the corresponding extracts and incubated at 37 °C in humidified air with 5 % CO_2. After 24 h of incubation, the samples were carefully rinsed with sterile PBS for 5 min, and kept in 100 µL of supplemented medium. Subsequently, the plates were incubated with 100 µL per well of a CellTiter-Glo 2.0 luminescence assay reagent and incubated for 15 min at room temperature with shaking. Finally, the luminescence (in Relative Light Units, RLUs) was measured using a spectrophotometer. The cell viability was calculated as:

$$Cell\ viability(\%) = \frac{RLU_S - RLU_B}{RLU_C - RLU_B}.100$$

where RLU_S, RLU_B, and RLU_C are the optical density for the sample (S), blank (culture medium) (B), and control (TCPS) (C), respectively. Regarding the statistical analysis, all experiments were carried out independently in triplicate and a minimum of three analyses per replication were performed. The significant differences in the experimental data were analyzed using the Student's *t*-test.

3. Results and discussion

3.1. Preparation and composition of the complex coacervates

The physical state of complex coacervates is typically quite sensitive to the method of preparation.[34] We prepared stoichiometric CHI-HA complex coacervates under vigorous stirring at pH 5, where both polyelectrolytes are almost fully charged.[32] After mixing all the components, the mixtures were left under stirring for 3 h to minimize heterogeneities due to kinetic trapping effects. We note that long stirring times do not necessarily eliminate kinetic trapping (basically, solid precipitates are kinetically trapped structures formed due to the strong association of the macroions leading to pairs with no or little exchange on observable time scales[35]), but ensures obtaining materials with reproducible properties. The samples were then allowed to rest for 24 h and centrifuged at 9500 rpm to separate the complex coacervate and the supernatant phases (Fig. 1).

The water content of the complex coacervate phase was measured via thermogravimetric analysis. The CHI-HA complex coacervates prepared at 0.1 to 0.45 M NaCl contained relatively large water contents (> 85 wt %), as shown in Fig. 2. Such values are characteristic of highly hydrophilic, water-rich complex coacervates.[7] At 0.5 M NaCl, the two phases (coacervate and supernatant) were difficult to distinguish with the naked eye and to separate from one another using a micropipette.

This indicates that this salt concentration is very close to the salt resistance of the system. At 0.55 M NaCl, no complexation between CHI and HA was observed using optical microscopy.

Previous works reported the salt resistance of this system to be 0.65 M NaCl at pH 4 [29] and pH 4.5 [28], and 0.55 M NaCl at pH 6 [29]. At first glance, this may be surprising given that the polymers used in our work are of higher molecular weights. However, the different preparation conditions in the previous reports (i.e. different pH values, 10 – 120 s of vortexing as opposed to 3 h of stirring, and centrifugation without rest time) may explain, at least to some extent, the moderately higher salt resistance.[28,29] Moreover, these works used CHI of relatively higher degrees of deacetylation. At comparable molecular weights, an increased degree of deacetylation is expected to promote macroion pairing per chain [32,36], thereby increasing the salt resistance. The fact that the salt resistance values are similar (0.55 to 0.65 M NaCl) in all these works (using CHI of various molecular weights) signifies the importance of CHI's degree of deacetylation in stabilizing these complex coacervates. Another point which can help to shed light on these apparent discrepancies is the total polymer concentration at which the CHI-HA complex coacervates were prepared in different reports. These concentrations do not necessarily correspond to the unique "critical" polymer and salt concentrations (at the maximum of the binodal curve). For example, in Es Sayyed's work [29], the total polymer concentration is at 24 mM (compare to 40 mM in Sun's work [28] and 39 mM in the present work).

As expected, the salt-induced increase in the water content (Fig. 2) is due to the doping effect of salt on the macroion pairs between the oppositely charged groups of HA and CHI.[37,38] Increasing the salt concentration reduces both the strength and the number of macroion pairs, favoring the swelling of the complex coacervate phase (see Fig. 1**C**), thereby decreasing the polymer concentration.[7] Yet, the high sensitivity of the CHI-HA system to a moderately doping salt (NaCl) is noticeable.[39] This sensitivity may be related to the lower charge densities of these polysaccharides compared to their synthetic counterparts such as poly(acrylic acid) (PAA) or polyallylamine (PAH), which bear the same ionizable functional groups.[32,40] A plausible consequence of this difference is a sparser network of macroion pairs (in a given volume) in the CHI-HA complex coacervates.[36]

3.2. Microscopic aspects of the complex coacervates

Before the mechanical investigations, we studied the microscopic aspects of the CHI-HA complex coacervates to visually assess their solid or liquid nature (Fig. 3). CHI-HA 0.1 and 0.2 M NaCl appeared as solid aggregates in the supernatant. The sample at 0.3 M NaCl appeared to be in a transition state, looking neither like solid precipitates nor like liquid

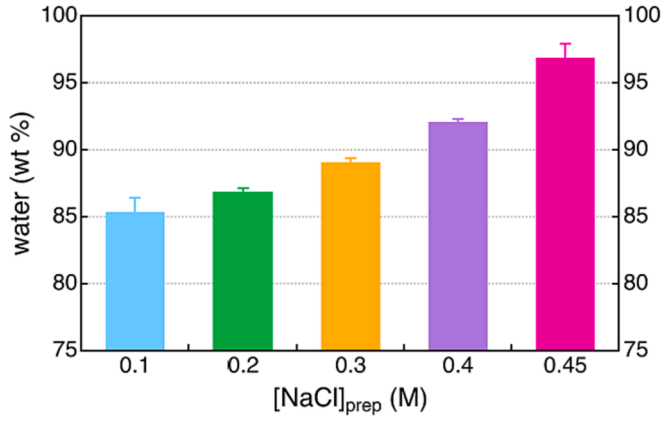

Fig. 2. The water content of the CHI-HA complex coacervate phase prepared at different NaCl concentrations. The error bars represent the standard deviation for three independently prepared and measured samples.

droplets. At 0.4 and 0.45 M NaCl, CHI-HA complex coacervates featured a liquid-like character, with abundant liquid droplets moving around in a pool of supernatant. In the case of CHI-HA 0.4 M NaCl, the droplets tend to coalesce, with some appearing as elongated, non-spherical features. This is likely due to their highly viscoelastic nature. Similar observations were reported for synthetic complex coacervates close to the critical gel point.[41] In the case of CHI-HA 0.45 M NaCl, the droplets were smaller in diameter (a few microns vs. tens of microns in the case of 0.4 M NaCl). This indicates a lower viscosity at 0.45 M NaCl, which allows more droplet breakup under the shear applied during the stirring. Complexation between CHI and HA still occurred at 0.5 M, but the droplets were barely distinguishable under the optical microscope (see Fig. 3). As mentioned earlier, and further verified by microscopic observations, we estimate the salt resistance to be around 0.55 M at pH 5.0. Sun et al. reported large, coalescing liquid droplets at 0.5 M NaCl at pH 4.5.[28] Qualitatively similar microscopic observations have been reported for other systems based on synthetic polyelectrolytes [41] and ionic polypeptides [42].

3.3. Predicting underwater adhesiveness via linear rheology

The salt-induced change in the composition of the complex coacervates (Figs. 1 and 2) and their microscopic aspects (Fig. 3) is known to modify their mechanical properties.[7,22,43] We seize this opportunity to fine-tune the rheological properties and thereby the underwater adhesiveness of CHI-HA complex coacervates. We first investigated the linear rheological behavior of the CHI-HA complex coacervates immersed in their supernatant at 37 °C. Fig. 4**A** shows the frequency dependence of the storage (G') and loss (G'') moduli for the samples prepared at different NaCl concentrations at pH 5.0. The corresponding loss factors ($tan(\delta) = G''/G'$) are shown in Fig. 4**B**. The rheological behavior of CHI-HA complex coacervates gradually transitions from viscoelastic solid-like (featuring the onset of a rubbery plateau at high frequencies) to viscoelastic liquid-like (typical of polymer solutions at low frequencies) at higher NaCl concentrations. Both G' and G'' decrease in magnitude and become increasingly frequency dependent, with their crossover shifting towards higher frequencies. This shift corresponds to shorter terminal relaxation times ($\tau_c = 1/\omega_c$), [44] indicating that the system becomes increasingly dynamic. At the highest salt concentration, the material exhibits the characteristic dynamics of a polymer solution in the terminal region, with G' and G'' scaling with ω^2 and ω^1, respectively (marked by the black and dark blue solid lines in Fig. 4**A**).

To investigate the viscoelastic behavior of these materials beyond the experimentally accessible window, we examined the applicability of the time-salt superposition principle. As shown in Fig. 4**C,** a master curve was obtained by shifting the original frequency sweeps (from Fig. 4**A**), taking the sample at 0.2 M NaCl as the reference. This indicates that the salt impacts all the relaxation modes to the same extent and that the material remains self-similar.[44,45] The horizontal shift factor (Fig. 4**D**) shows a strong dependence on salt concentration, changing by 3 decades when the NaCl concentration is increased from 0.1 to 0.45 M. The fit, marked by the dashed line, represents the following scaling, $a_S \propto \exp(A - B.[NaCl])$, with A and B constants, as found in other systems. [22,46] The vertical shift factor has a weak dependence on salt concentration, accounting for the change in polymer volume fraction. These trends are in good agreement with previous reports.[28,29]

Except for some differences, previous reports on CHI-HA complex coacervates at pH 4 and 4.5 have found generally similar trends to those in the present work. In comparison to the work of Sun and co-workers [28] (polysaccharides of comparable molecular weights to this work, pH 4.5), we find relatively lower dynamic moduli at identical salt concentrations. Moreover, our complex coacervates are more sensitive to the increase in salt concentration as the transition between the viscoelastic solid-like and the viscoelastic liquid-like behaviors occurs around

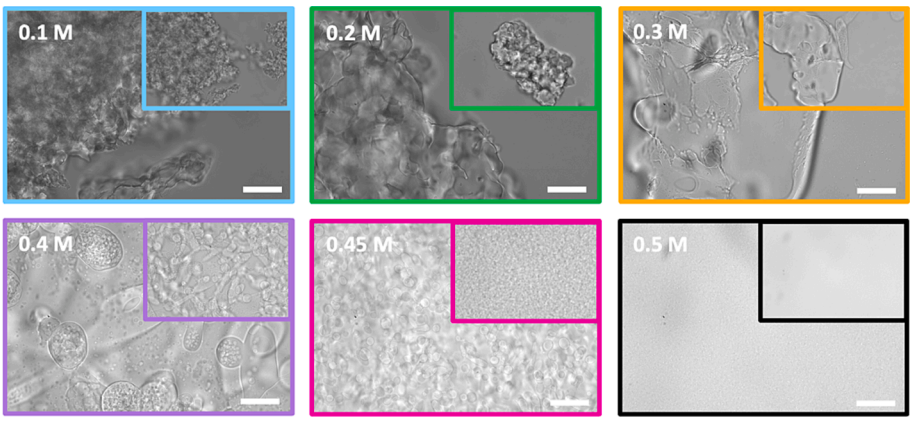

Fig. 3. Typical optical microscopy images of the complex coacervates after 1 h of mixing. The scale bars at the bottom right of the images mark 20 μm.

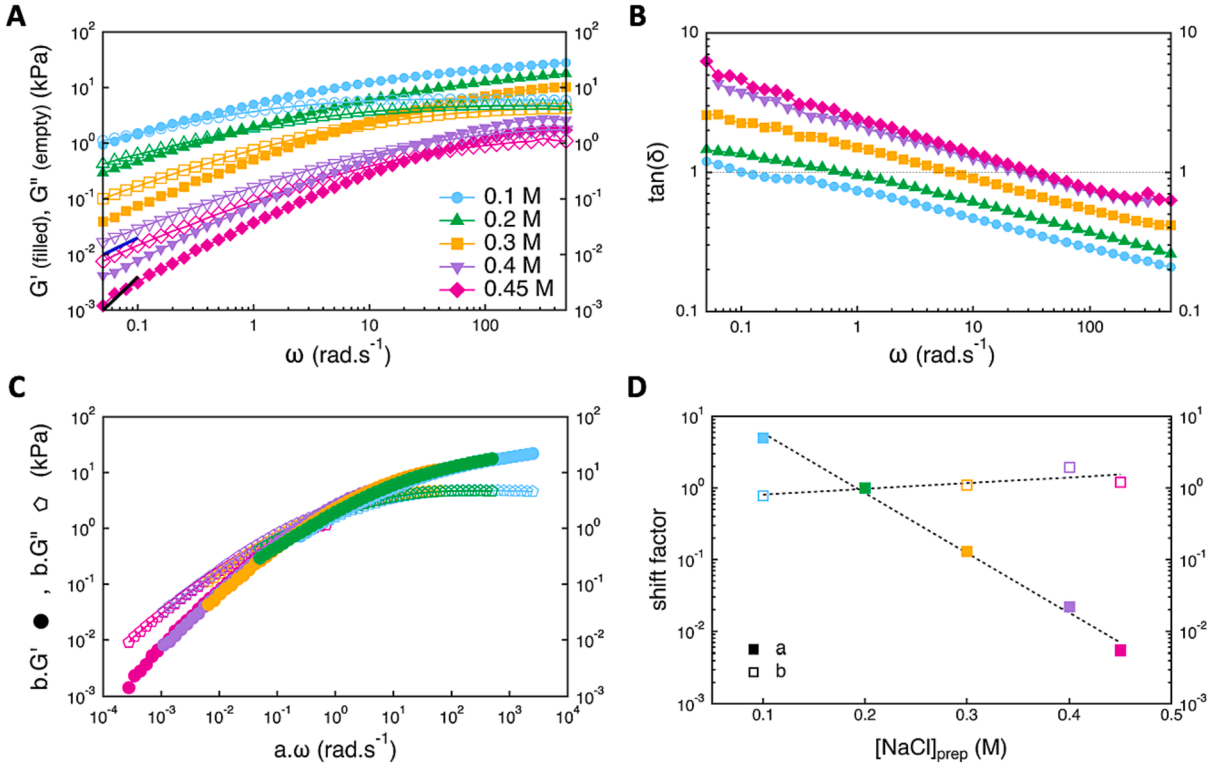

Fig. 4. Linear viscoelastic properties of the CHI-HA complex coacervates at 37 °C: (A) storage modulus ($G^{'}$), loss modulus ($G^{''}$), and (B) the loss factor, $tan(\delta) = G^{''}/G^{'}$ as a function of angular frequency. The black and dark blue lines on A mark $\propto\omega^2$ and $\propto\omega^1$, respectively. All the samples were tested in their respective supernatant. (C) Dynamic moduli master curve constructed through time-salt superposition. (D) The dependence of the *a*, horizontal, and *b*, vertical, shift factors on the preparation NaCl concentration.

0.3 M, as opposed to 0.5 M in the work of Sun. On the other hand, Es Sayed and colleagues reported viscoelastic liquid-like coacervates (low molecular weight (30 – 50 kg.mol^{-1}) polysaccharides at pH 4), even in the absence of added salt.[29] In making these *qualitative* comparisons, we note that the preparation methods, polymer molecular weights, pH values, and total salt and polymer concentrations can each impact the viscoelastic properties of these water-rich materials.

Importantly, as witnessed by the construction of a master curve through a time-salt superposition (see Fig. 4**C**), the fact that our CHI-HA complex coacervates remain self-similar at all the salt concentrations studied confirms that the dynamics of these materials is mainly controlled by electrostatics. In other words, dynamically arrested domains reported for this system at pH 6 [29] are not present or significant enough at pH 5 where both polymers are still almost fully charged [32].

We now analyze these results to predict which samples are expected to have the best underwater adhesive performance. Considering the general requirements discussed in the introduction, the sample at 0.1 M is expected to be the stickiest, followed by the sample at 0.2 M. As seen in Fig. 4, CHI-HA 0.1 and 0.2 M samples exhibit the onset of a rubbery plateau with a terminal relaxation time of 10.0 and 1.4 s, respectively. This behavior, with a plateau modulus on the order of several kPa (well below the Dahlquist's criterion of 0.1 MPa [17]), is typical of highly viscoelastic polymer liquids. [28,17] Moreover, the values of $tan(\delta)$ for these two samples fall in the range of 0.3 – 1 on the time scales relevant for typical adhesion experiments (10^{-2} – 10^{1} s).[7] Furthermore, these two samples have the lowest water contents among the samples studied (Fig. 2). The coacervates prepared at 0.3, 0.4, and 0.45 M NaCl have higher water contents and increasingly liquid-like behavior, making

them potentially weaker underwater adhesives.

We also characterized the rheological properties of the different CHI-HA coacervates upon a salt switch in 0.1 M NaCl at 37 °C, as a model medium for physiological conditions. Due to the pH-sensitive nature of these materials and the formation of hydrogen bonds at higher pH [29], we decided to first determine the role of a salt switch alone. Therefore, the pH of the immersion medium was kept at pH 5.0. The real-time evolution of the dynamic moduli and the loss factor of the samples over 1 h of the salt switch are shown in Fig. 5**A** and **B**, respectively. It should be emphasized that the measured change in the mechanical properties is an average value, as the switch starts at the periphery of the confined disk and advances toward the center.

In the case of CHI-HA 0.1 M NaCl, no salt switch takes place due to the absence of a gradient in salt concentration and the material remains stable in this medium. The samples prepared at higher salt concentrations show an increase in their dynamic moduli as soon as they are immersed in 0.1 M NaCl. This is due to the formation of additional macroion pairs as the salt diffuses out of the complex coacervates. The liquid-like CHI-HA coacervates undergo a sol–gel transition followed by gradual hardening, while the solid-like samples harden into stronger and increasingly elastic-like solids. This behavior is concomitant with the drop in $tan(\delta)$ to values between 0.3 and 0.5 within 1 h.

Except for the 0.1 M sample which does not undergo a salt switch, all the other samples are expected to have improved underwater adhesion after the salt switch, compared to when they were immersed in their supernatant. The advantage of this strategy is that the material can make good contact in its initial liquid-like or soft state, and further solidify and harden *in-situ*. Among the different CHI-HA complex coacervates, the sample at 0.2 M is expected to have an optimal performance in phosphate-buffered saline (0.137 M NaCl, pH 7.4) as a model of the physiological environment. Upon immersion in PBS, this complex coacervate undergoes two opposing changes: (i) a salt switch as the NaCl concentration decreases to 0.137 M and (ii) a pH switch as the pH increases to 7.4. The salt switch tends to solidify the material, as seen in Fig. 5, while the pH switch is expected to eventually soften and possibly dissociate the material as CHI gradually becomes uncharged.

The evolution of the dynamic moduli of CHI-HA 0.2 M NaCl coacervates as a function of immersion time in PBS is shown in **Figure S1**. During the first 90 min, the dynamic moduli increase slightly. Longer immersion times result in a moderate decrease in the dynamic moduli up to 9 h, followed by a more rapid softening. Notably, the material is still solid-like with a storage modulus at half the initial value after 35 h in PBS. These results suggest that the salt switch occurs on relatively shorter time scales (1 h) compared to the pH switch (10 h). We verified this by performing independent experiments, changing one parameter at a time: (i) by changing the pH from 5 to pH 7.4 in 0.2 M NaCl and (ii) by changing the salt concentration from 0.2 M to 0.137 M NaCl at pH 5.0. The results are shown in **Figure S2**. It should also be noted that the contribution of hydrogen bonding to the mechanical properties of this material becomes significant as the increase in pH causes the deionization of CHI.[29] This can partly explain the slower response of the material to an increase in pH (**Figure S2**); a feature that should favor the prolonged performance of the material under physiological conditions. Another possibility to explain the slower kinetics of the pH-triggered changes in rheology is the buffering capacity of the coacervate itself. [47,48]

3.4. Adhesion in aqueous and physiological media

Considering the viscoelastic behavior of CHI-HA complex coacervates in aqueous media, we proceeded to study their adhesive behavior in underwater pull-off tests as previously described.[33] Following the same order as the previous section, we first studied the underwater adhesiveness of each complex coacervate in its supernatant. In a second set of experiments, the adhesiveness of the complex coacervates was studied after a salt switch in a large volume of 0.1 M NaCl at pH 5 or in PBS (0.137 M NaCl at pH 7.4). Typical nominal stress – strain curves are provided in **Figure S3**.

The filled bars in Fig. 6 present the average underwater strength values for CHI-HA complex coacervates in their supernatant. The softening effect of the salt on the complex coacervates is visible from the decrease in adhesion strength. In the case of CHI-HA 0.1 and 0.2 M NaCl, the average adhesion strengths (in pull-off) are 44.4 and 40.3 kPa in their respective supernatant. At higher salt concentrations, the values drop rather abruptly, down to 1.3 kPa at 0.45 M NaCl. These are the adhesive strengths of the CHI-HA complex coacervates without any external triggers such as temperature, salt concentration, or pH.

Quantitative comparisons between the linear rheology and the pull-off data are not straightforward.[49] Nonetheless, the salt-dependent trend in the adhesion strength (Fig. 6, filled bars) is in excellent agreement with our predictions based on the linear viscoelastic behavior of these materials in their supernatant (Fig. 4). To further elucidate the trend in adhesion strength, we used the following approximation, $\omega_{deb} \approx 2\pi V_{deb}/h_0$, to link the time scale of the pull-off test to the corresponding angular frequency from linear rheology. V_{deb} and h_0 are the debonding rate (100μ m.s^{-1}) and the initial thickness of the layer (500μ m), respectively.[20] In our experiments, the corresponding angular frequency is $\omega_{deb} = 1.25$ rad.s^{-1}. This frequency is just above the crossover frequency of the CHI-HA 0.2 M NaCl sample (0.70 rad.s^{-1}) and below that of the 0.3 M NaCl sample (3.15 rad.s^{-1}). Based on this rough approximation, the 0.2 M NaCl sample is expected to be less dynamic and more viscoelastic on the time scale of the pull-off test. This explains the abrupt drop of the adhesion strengths (filled bars in Fig. 6) at NaCl concentrations above 0.2 M.

The underwater adhesion strengths of the complex coacervates undergoing a salt switch in 0.1 M NaCl at pH 5 are given by the hatched

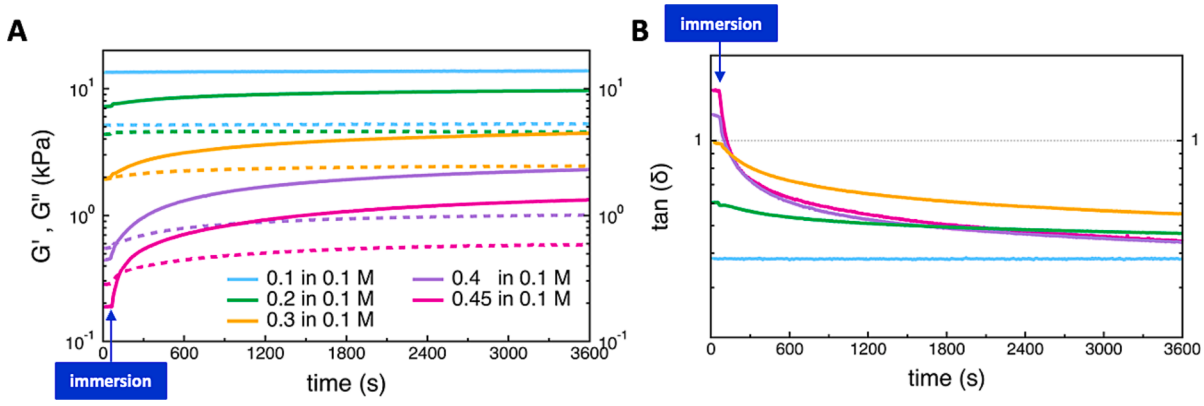

Fig. 5. Time sweep data (at 10 rad.s^{-1}) of CHI-HA complex coacervates upon immersion in 0.1 M NaCl at pH 5.0 (A) Storage (G') and loss (G'') moduli. (B) $tan(\delta)$.

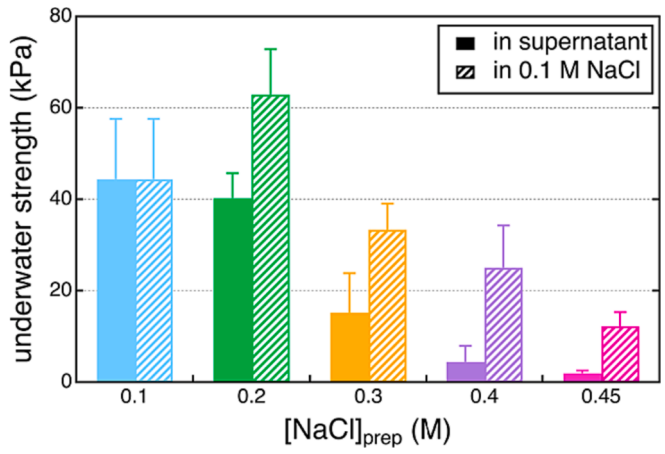

Fig. 6. Underwater adhesion strength of the CHI-HA complex coacervates in their supernatant and upon 1 h of salt switch in 0.1 M NaCl at pH 5.0. The pull-off tests were performed at 37 °C at a nominal strain rate of 0.2 s^{-1}.

bars in Fig. 6. Generally, a significant increase is observed compared to the values measured in the case of the coacervates in their supernatant (filled bars). We recall that the CHI-HA 0.1 M does not experience a switch. Once more, the improved adhesion strength of the hardened complex coacervates is in good agreement with the increase in their dynamic moduli upon salt switch (Fig. 5). An intriguing observation is that the adhesion strength of the 0.2 M NaCl sample after 1 h of salt switch in a 0.1 M NaCl (62.9 kPa) is even higher than that of the sample prepared in 0.1 M NaCl (44.4 kPa).

To explain this point, we study the quality of the initial contact and the evolution of the viscoelastic properties during the course of the salt switch. At the time of contact formation, CHI-HA 0.1 M and 0.2 M NaCl have $tan(\delta)$ values of 0.4 and 0.6, respectively (Fig. 5). This means that the 0.2 M NaCl sample is a more viscoelastic material (closer to the gel point) and therefore able to make better contact with the substrate. This sample is also relatively softer (lower G') than the 0.1 M NaCl sample. Over the course of the salt switch, CHI-HA 0.2 M NaCl sample gradually hardens but its final loss factor remains larger than that of the sample at 0.1 M NaCl, while its storage modulus remains slightly lower (Fig. 5). As such, one might argue that the CHI-HA coacervate at 0.3 M NaCl (and higher NaCl concentrations) should form even better contacts with the probe, given their relatively larger values of $tan(\delta)$. This argument is indeed valid, which is why a more comprehensive explanation is needed that considers both $tan(\delta)$ and G'.

Deplace and coworkers [20] suggested that for a given geometry and substrate, there is an optimal window of $tan(\delta)/G'$ where the material is capable of both forming a good contact and resisting debonding. Outside this window of $tan(\delta)/G'$ (at the angular frequency equivalent to the strain rate of the pull-off test), the material is either too solid-like and stiff to be able to form good contact (too low $tan(\delta)/G'$) or too liquid-like to resist debonding (too high $tan(\delta)/G'$). Accessing this window by crossing the lower threshold of $tan(\delta)/G'$, a transition from interfacial crack propagation to fibrillation is expected. In other words, relatively higher values of $tan(\delta)/G'$ indicate a stronger interface (regardless of the eventual type of failure; adhesive or cohesive). In our experiments, both CHI-HA 0.1 M and 0.2 M NaCl detach adhesively from the probe. However, the initial value of $tan(\delta)/G'$ is higher for the 0.2 M NaCl sample (8.3×10^{-5} Pa^{-1}) compared to that of the 0.1 M NaCl sample (2.8×10^{-5} Pa^{-1}). Therefore, this approximation predicts a stronger interface in the case of CHI-HA 0.2 M NaCl coacervates, consistent with its higher adhesion strength (Fig. 6).

As shown in **Figure S4**, over the course of the salt switch, the value of $tan(\delta)/G'$ decreases as CHI-HA 0.2 M NaCl becomes more solid-like, but it remains larger than that of the 0.1 M NaCl sample after 1 h. Lower values of $tan(\delta)/G'$ (which is equal to G''/G'^2) can be due to either a relative decrease in G'' or a relative increase in G', knowing that changes in G' have a greater impact (as G' is squared). In our case, both G'' and G' increase during the course of the salt switch (Fig. 5), with a concomitant reduction in $tan(\delta)$. This means that G' increases at a higher rate than G'', rendering the material less viscoelastic and less dynamic. Therefore, while a relatively higher *initial* value of $tan(\delta)/G'$ ensures better contact formation, relatively lower *final* values of $tan(\delta)/G'$ are needed for greater resistance to debonding. In fact, values below a critical value of $tan(\delta)/G'$ lead to premature detachment. We remind the reader that the adhesion of soft materials strongly depends on both contact formation and resistance to debonding.[49] In light of these explanations, the ideal transition would be rapid, with a change in $tan(\delta)/G'$ from very high to near-critical, low values, with the material transitioning from a low-viscosity liquid to a *robust, viscoelastic* (but not too elastic) solid.

Regarding the type of failure in the case of CHI-HA 0.1 and 0.2 M NaCl, no fibrillation was observed under the experimental conditions of this work (with maximum strains below 100 %). For fibrillation to occur, the viscoelastic response of the material must be near the entanglement relaxation time (well within the rubbery plateau) on the time scale of the pull-off test. However, the viscoelastic response of the CHI-HA complex coacervates is close to their *terminal* relaxation time. We therefore anticipate that fibrillation should occur in pull-off tests performed at strain rates two decades above the current value (i.e. in the range of 2 – 20 s^{-1}). In any case, a clean detachment without fibrillation is not a drawback for the intended applications of this work.

CHI-HA 0.2 M NaCl has a slightly lower adhesion strength of 50 kPa in PBS when compared to 62.9 kPa when tested in 0.1 M NaCl at pH = 5. This is expected from the time sweeps in PBS (see **Figure S1**). Moreover, the adhesion strengths measured at different immersion times in PBS remained relatively constant for up to 24 h. As mentioned earlier, this is most likely due to the added contribution of the hydrogen bonds, which compensate the loss of properties as CHI loses its charge at higher pH. These features make the CHI-HA complex coacervate at 0.2 M NaCl an ideal candidate for potential biomedical applications.

The adhesion strength of the CHI-HA 0.2 M NaCl (40 – 63 kPa depending on the test medium, see Fig. 6) is comparable to the highest values reported for *water-rich*, complex coacervates based on model polyelectrolytes tested under comparable experimental conditions.[7] For example, the complex coacervates of poly(2-acrylamido-2-methylpropanesulfonic acid) and poly(N,N-[(dimethylamino) propyl] methacrylamide) had a maximum adhesion strength of 24 kPa in 0.1 M NaCl (at a rate of 0.2 s^{-1}).[24] In another work, an adhesion strength of 7 kPa was reported for complex coacervates of poly(acrylic acid) and poly(N,*N*-dimethylaminopropyl acrylamide).[50] The highest adhesion strength reported here is also comparable to those of other systems based on H-bonding and hydrophobic interactions.[21,33,51,52] In particular, Dompé and colleagues measured adhesion strengths of 60 kPa for thermoresponsive complex coacervates with a reduced water content of 77 wt% (after extrusion) by adjusting the temperature and the salt concentration of the medium.[52] The added values of the CHI-HA complex coacervates reported here are that they are bio-sourced, water-rich, and potentially less toxic than synthetic polyelectrolytes.

3.5. Antibacterial and cytocompatibility of CHI-HA

Bioactive, biodegradable, and potentially less toxic than synthetic polyelectrolytes, CHI-HA complex coacervates are promising candidates as biomedical adhesives. Since CHI is known to be antibacterial, we first investigate the antibacterial property of CHI-HA 0.2 M NaCl against Gram-positive *Staphylococcus aureus* (*S. aureus*) and Gram-negative *Escherichia coli* (*E. coli*). Bacterial quantification (in colony forming unit per mL, CFU/mL) was performed after 24 h incubation with the sample and TCPS substrate as a control (Ctrl) (Fig. 7). CHI-HA 0.2 M

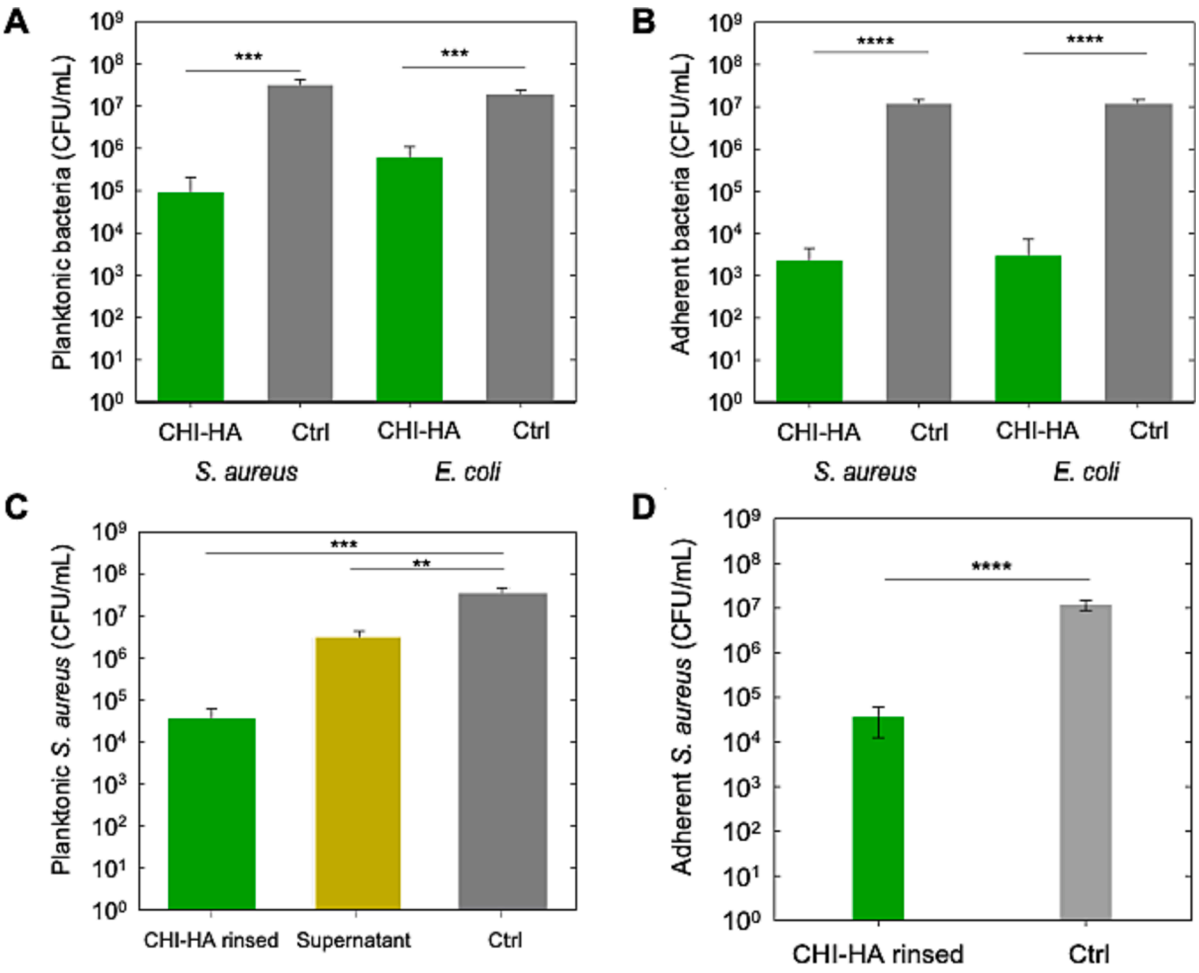

Fig. 7. Microbiological tests on CHI-HA 0.2 M NaCl coacervates. Colony-forming unit (CFU) of (A, C) planktonic (B, D) adherent *S. aureus* and *E. coli* cells incubated for 24 h in contact with (A, B) CHI-HA coacervates and (C, D) rinsed CHI-HA coacervates with the supernatant retrieved at the rinsing. TCPS was used as control (Ctrl). The differences between the given groups were tested for statistical significance using Student's *t*-test (**p < 0.01; ***p < 0.001; ****p < 0.0001).

NaCl coacervates showed a significant reduction of both tested bacterial strains in the planktonic state, i.e. present in the supernatant. A stronger efficacy was observed against *S. aureus* with a reduction of more than 2.5 $\log_{10}$ (99.7 %) vs 1.5 $\log_{10}$ (96.7 %) against *E. coli*. Adherent bacteria on CHI-HA coacervates were harvested from the surfaces by ultrasonication to evaluate their viability (Fig. 7**B**). A reduction of 3.7 $\log_{10}$ (99.98 %) against *S. aureus* and *E. coli* was observed in comparison to the Ctrl. These results confirmed the antibacterial properties of CHI-HA coacervates. CHI is known to interact with the negatively charged bacterial cell wall through electrostatic interactions, causing the permeabilization of the bacterial surface, the leakage of intracellular substances, and subsequently the death of the bacteria. [26] To explore the mechanism of action, the CHI-HA coacervates were rinsed with the culture medium for 24 h prior to bacterial incubation and tested against *S. aureus* as well as the collected supernatant. Rinsed coacervates present similar bacterial reduction in planktonic (2.9 $\log_{10}$, 99.9 %) and adherent bacteria 2.7 $\log_{10}$ (99.7 %) compared to non-rinsed coacervates (Fig. 7**C**). In the case of the collected supernatant, the bacterial reduction was 1 $\log_{10}$ (90.4 %), probably due to the presence of CHI in the supernatant. In agreement with the decrease of rheological properties of the coacervates upon contact with PBS, these results provide evidence for the release of CHI chains (as well as HA) in the supernatant from the CHI-HA coacervates. Moreover, if CHI chains are chemically crosslinked to HA by a carbodiimide reaction, the antibacterial activity of the CHI-HA coacervates is lost (**Figure S5 A**). [22]

Finally, the cytotoxicity of the CHI-HA coacervates was assessed on BALB 3 T3 mouse fibroblast cells, using the CellTiter-Glo 2.0 indirect luminescence test, which indicates the metabolic activity of cells. Cell viability was evaluated after 24 h of incubation with the extraction fluid of CHI-HA 0.2 M NaCl coacervates (**Figure S5 B**). There is no significant difference in the cell viability found compared to cells in contact with the culture medium, indicating that the CHI-HA complex coacervates are noncytotoxic.

4. Conclusions

We have fine-tuned the underwater adhesive properties of non-cytotoxic and antibacterial complex coacervates from bio-sourced polysaccharides, CHI and HA. We found that the water content of these complex coacervates is extremely high (>85 wt%) and very sensitive to small variations in NaCl concentration. The viscoelastic properties of these complex coacervates were tuned via salt-induced changes in their composition, notably their water content. By studying the viscoelastic properties of these complex coacervates, we predicted that the coacervates prepared near physiological salt concentrations (0.1 and 0.2 M NaCl) should be inherently sticky, without the need for an external trigger or switch. This prediction was validated by well-controlled pull-off experiments on complex coacervates immersed in their own supernatant.

We also studied CHI-HA complex coacervates after a salt switch in 0.1 M NaCl at pH = 5.0 and a combined salt *and* pH switch in phosphate-buffered saline (0.137 M NaCl, pH = 7.4). As expected from the

evolution of the viscoelastic properties of the complex coacervates experiencing a salt switch, the underwater adhesion strength was systematically enhanced. The highest underwater adhesion strength of 62.9 kPa was obtained with CHI-HA 0.2 M NaCl after 1 h of salt switch at 37 °C. This adhesion strength is one of the highest reported values for *water-rich* underwater adhesives based on complex coacervates. We also showed that this material maintains 80 % of its adhesion strength after 24 h of immersion in phosphate-buffered saline. This was associated with the slight reduction in the dynamic moduli due to the trade-off between (i) the deionization of CHI at pH 7.4, effectively reducing the transient crosslink density, and (ii) the formation of dynamically-arrested domains due to hydrogen bonding [29].

To summarize, the key advantages of the reported CHI-HA coacervates over current coacervate-based underwater and biomedical adhesives are that (i) they are based on bio-sourced polymers, (ii) they are prepared via a simple mixing method, (iii) they combine significant water contents (> 85 wt %) and underwater pull-off adhesion strengths comparable to some the highest values (5 – 90 kPa) reported for *chemically crosslinked* tissue adhesives based on either CHI or HA, (iv) they do not require a large trigger to perform, and (v) they are inherently antibacterial and non-cytotoxic. The present work highlights the untapped potential of simple, bio-sourced complex coacervates for future biomedical applications.

CRediT authorship contribution statement

Perrine Galland: Writing – review & editing, Writing – original draft, Methodology, Investigation, Formal analysis, Data curation. **Muhammad Haseeb Iqbal:** Writing – review & editing, Validation, Methodology, Formal analysis, Data curation, Conceptualization. **Damien Favier:** Methodology, Formal analysis, Data curation. **Mélanie Legros:** Methodology, Formal analysis, Data curation. **Pierre Schaaf:** Writing – review & editing, Validation, Supervision, Funding acquisition, Conceptualization. **Fouzia Boulmedais:** Writing – review & editing, Writing – original draft, Validation, Supervision, Resources, Project administration, Funding acquisition, Formal analysis, Conceptualization. **Mehdi Vahdati:** Writing – review & editing, Writing – original draft, Validation, Supervision, Software, Resources, Project administration, Investigation, Funding acquisition, Formal analysis, Data curation, Conceptualization.

Declaration of competing interest

The authors declare the following financial interests/personal relationships which may be considered as potential competing interests: Fouzia Boulmedais reports financial support was provided by Carnot Institute MICA. Fouzia Boulmedais reports financial support was provided by Fonds Régional de Coopération pour la Recherche of Région Grand Est. Fouzia Boulmedais reports financial support was provided by Jean-Marie Lehn Foundation. Fouzia Boulmedais and Mehdi Vahdati report financial support was provided by Interdisciplinary Institute HiFunMat.

Data availability

Data will be made available on request.

Acknowledgements

The authors gratefully acknowledge Institut Carnot MICA (MATRIX project), Fonds Régional de Coopération pour la Recherche of Région Grand Est (ERMES project), and Fondation Jean-Marie Lehn (THEOS project) for financial support. This work of the Interdisciplinary Institute HiFunMat, as part of the ITI 2021-2028 program of the University of Strasbourg, CNRS and Inserm, was supported by IdEx Unistra (ANR-10-IDEX-0002) and SFRI (STRAT'US project, ANR-20-SFRI-0012) under the framework of the French Investments for the Future Program. The authors would like to thank Stéphane Trombotto (IMP, Université Claude Bernard Lyon 1, UMR CNRS 5223) for detailed analysis of chitosan via SEC and ^{1}H-NMR, as well as Quentin Bailleul and Leandro Jacomine (CNRS, Institut Charles Sadron) for fruitful discussions. The CarMac facility of ICS is acknowledged for TGA experiments.

Appendix A. Supplementary material

Supplementary data to this article can be found online at https://doi.org/10.1016/j.jcis.2024.01.193.

References

[1] T. Zhu, J. Mao, Y. Cheng, H. Liu, L. Lv, M. Ge, S. Li, J. Huang, Z. Chen, H. Li, L. Yang, Y. Lai, Recent progress of polysaccharide-based hydrogel interfaces for wound healing and tissue engineering, Adv. Mater. Interfaces 6 (17) (2019), https://doi.org/10.1002/admi.201900761.

[2] H.E. Caputo, J.E. Straub, M.W. Grinstaff, Design, synthesis, and biomedical applications of synthetic sulphated polysaccharides, Chem. Soc. Rev. 48 (8) (2019) 2338–2365, https://doi.org/10.1039/c7cs00593h.

[3] Z. Ma, G. Bao, J. Li, Multifaceted design and emerging applications of tissue adhesives, Adv. Mater. 33 (2021) 2007663, https://doi.org/10.1002/adma.202007663.

[4] C. Ghobril, M.W. Grinstaff, The chemistry and engineering of polymeric hydrogel adhesives for wound closure: A tutorial, Chem. Soc. Rev. 44 (7) (2015) 1820–1835, https://doi.org/10.1039/c4cs00332b.

[5] F. Scognamiglio, A. Travan, I. Rustighi, P. Tarchi, S. Palmisano, E. Marsich, M. Borgogna, I. Donati, N. De Manzini, S. Paoletti, Adhesive and sealant interfaces for general surgery applications, J. Biomed. Mater. Res. B Appl. Biomater. 104 (3) (2016) 626–639, https://doi.org/10.1002/jbm.b.33409.

[6] D.M. Fitzgerald, Y.L. Colson, M.W. Grinstaff, Synthetic pressure sensitive adhesives for biomedical applications, Prog. Polym. Sci. (2023) 101692, https://doi.org/10.1016/j.progpolymsci.2023.101692.

[7] M. Vahdati, D. Hourdet, C. Creton, Soft underwater adhesives based on weak molecular interactions, Prog. Polym. Sci. 139 (2023) 101649, https://doi.org/10.1016/j.progpolymsci.2023.101649.

[8] E. Lih, J.S. Lee, K.M. Park, K.D. Park, Rapidly curable chitosan-PEG hydrogels as tissue adhesives for hemostasis and wound healing, Acta Biomater. 8 (9) (2012) 3261–3269, https://doi.org/10.1016/j.actbio.2012.05.001.

[9] M. Lu, Y. Liu, Y.C. Huang, C.J. Huang, W.B. Tsai, Fabrication of photo-crosslinkable glycol chitosan hydrogel as a tissue adhesive, Carbohydr. Polym. 181 (2018) 668–674, https://doi.org/10.1016/j.carbpol.2017.11.097.

[10] X. Du, Y. Liu, H. Yan, M. Rafique, S. Li, X. Shan, L. Wu, M. Qiao, D. Kong, L. Wang, Anti-infective and pro-coagulant chitosan-based hydrogel tissue adhesive for sutureless wound closure, Biomacromolecules 21 (3) (2020) 1243–1253, https://doi.org/10.1021/acs.biomac.9b01707.

[11] N.D. Sanandiya, S. Lee, S. Rho, H. Lee, I.S. Kim, D.S. Hwang, Tunichrome-inspired pyrogallol functionalized chitosan for tissue adhesion and hemostasis, Carbohydr. Polym. 208 (2019) 77–85, https://doi.org/10.1016/j.carbpol.2018.12.017.

[12] D. Bermejo-Velasco, S. Kadekar, M.V. Tavares Da Costa, O.P. Oommen, K. Gamstedt, J. Hilborn, O.P. Varghese, First aldol cross-linked hyaluronic acid hydrogel: Fast and hydrolytically stable hydrogel with tissue adhesive properties, ACS Appl. Mater. Interfaces 11 (41) (2019) 38232–38239, https://doi.org/10.1021/acsami.9b10239.

[13] D. Wang, P. Xu, S. Wang, W. Li, W. Liu, Rapidly curable hyaluronic acid-catechol hydrogels inspired by scallops as tissue adhesives for hemostasis and wound healing, Eur. Polym. J. 134 (2020), https://doi.org/10.1016/j.eurpolymj.2020.109763.

[14] D. Zhou, S. Li, M. Pei, H. Yang, S. Gu, Y. Tao, D. Ye, Y. Zhou, W. Xu, P. Xiao, Dopamine-modified hyaluronic acid hydrogel adhesives with fast-forming and high tissue adhesion, ACS Appl. Mater. Interfaces 12 (16) (2020) 18225–18234, https://doi.org/10.1021/acsami.9b22120.

[15] N. Pandey, L. Soto-Garcia, S. Yaman, A. Kuriakose, A.U. Rivera, V. Jones, J. Liao, P. Zimmern, K.T. Nguyen, Y. Hong, Polydopamine nanoparticles and hyaluronic acid hydrogels for mussel-inspired tissue adhesive nanocomposites, Mater. Sci. Eng. C (2021), https://doi.org/10.1016/j.msec.2021.112589.

[16] H. Gao, C. Yu, Q. Li, X. Cao, Injectable DMEM-induced phenylboronic acid-modified hyaluronic acid self-crosslinking hydrogel for potential applications in tissue repair, Carbohydr. Polym. 258 (2021), https://doi.org/10.1016/j.carbpol.2021.117663.

[17] C.A. Dahlquist. Pressure-Sensitive Adhesives. In *Treatise on Adhesion and Adhesives*; Patrick, R. L., Ed.; Marcel Dekker, Inc., 1969; pp 219–260. https://doi.org/https://doi.org/10.1002/app.1969.070130622.

[18] A. Zosel, Adhesion and tack of polymers: influence of mechanical properties and surface tensions, Colloid Polym. Sci. 263 (7) (1985) 541–553, https://doi.org/10.1007/BF01421887.

[19] B.E. Gdalin, E.V. Bermesheva, G.A. Shandryuk, M.M. Feldstein, Effect of temperature on probe tack adhesion: Extension of the Dahlquist criterion of tack, J. Adhes. 87 (2) (2011) 111–138, https://doi.org/10.1080/00218464.2011.545325.

[20] F. Deplace, C. Carelli, S. Mariot, H. Retsos, A. Chateauminois, K. Ouzineb, C. Creton, Fine tuning the adhesive properties of a soft nanostructured adhesive with rheological measurements, J. Adhes. 85 (1) (2009) 18–54, https://doi.org/10.1080/00218460902727381.
[21] Y.J. Wang, Y. He, S.Y. Zheng, Z. Xu, J. Li, Y. Zhao, L. Chen, W. Liu, Polymer pressure-sensitive adhesive with a temperature-insensitive loss factor operating under water and oil, Adv. Funct. Mater. 2104296 (2021) 1–8, https://doi.org/10.1002/adfm.202104296.
[22] K.R. Shull, Z. Jiang, Q. Wang, B. Keshavarz, Y. Chen, K. Sadman, Influence of hydrophobicity on polyelectrolyte complexation, Macromolecules 50 (23) (2017) 9417–9426, https://doi.org/10.1021/acs.macromol.7b02031.
[23] M. Dompé, F.J. Cedano-Serrano, M. Vahdati, L. van Westerveld, D. Hourdet, C. Creton, J. van der Gucht, T. Kodger, M. Kamperman, Underwater adhesion of multiresponsive complex coacervates, Adv. Mater. Interfaces 7 (4) (2020) 1901785, https://doi.org/10.1002/admi.201901785.
[24] M. Vahdati, F.J. Cedano Serrano, C. Creton, D. Hourdet, Coacervate-based underwater adhesives in physiological conditions, ACS Appl. Polym. Mater. 2 (2020) 3397–3410, https://doi.org/10.1021/acsapm.0c00479.
[25] J.P. Jones, M. Sima, R.G. O'Hara, R.J. Stewart, Water-borne endovascular embolics inspired by the undersea adhesive of marine sandcastle worms, Adv. Healthc. Mater. 5 (7) (2016) 795–801, https://doi.org/10.1002/adhm.201500825.
[26] J. Li, S. Zhuang, Antibacterial activity of chitosan and its derivatives and their interaction mechanism with bacteria: Current state and perspectives, Eur. Polym. J. 138 (2020) 109984, https://doi.org/10.1016/j.eurpolymj.2020.109984.
[27] T.C. Laurent. *The Chemistry, Biology, and Medical Applications of Hyaluronan and Its Derivatives*; Portland Pr, 1998. https://doi.org/https://doi.org/10.1021/jm980609z.
[28] J. Sun, J.D. Schiffman, S.L. Perry, Linear viscoelasticity and time-alcohol superposition of chitosan/hyaluronic acid complex coacervates, ACS Appl. Polym. Mater. 4 (3) (2022) 1617–1625, https://doi.org/10.1021/acsapm.1c01411.
[29] J. Es Sayed, C. Caïto, A. Arunachalam, A. Amirsadeghi, L. van Westerveld, D. Maret, R.A. Mohamed Yunus, E. Calicchia, O. Dittberner, G. Portale, D. Parisi, M. Kamperman, Effect of dynamically arrested domains on the phase behavior, linear viscoelasticity and microstructure of hyaluronic acid – chitosan complex coacervates, Macromolecules 56 (15) (2023) 5891–5904, https://doi.org/10.1021/acs.macromol.3c00269.
[30] W. Tang, J. Wang, H. Hou, Y. Li, J. Wang, J. Fu, L. Lu, D. Gao, Z. Liu, F. Zhao, X. Gao, P. Ling, F. Wang, F. Sun, H. Tan, Review: Application of chitosan and its derivatives in medical materials, Int. J. Biol. Macromol. (2023), https://doi.org/10.1016/j.ijbiomac.2023.124398.
[31] M. Dovedytis, Z.J. Liu, S. Bartlett, Hyaluronic acid and its biomedical applications: A review, Eng. Regen. (2020) 102–113, https://doi.org/10.1016/j.engreg.2020.10.001.
[32] A.B. Kayitmazer, A.F. Koksal, E. Kilic Iyilik, Complex coacervation of hyaluronic acid and chitosan: Effects of PH, ionic strength, charge density, chain length and the charge ratio, Soft Matter 11 (44) (2015) 8605–8612, https://doi.org/10.1039/c5sm01829c.
[33] M. Vahdati, G. Ducouret, C. Creton, D. Hourdet, Thermally triggered injectable underwater adhesives, Macromol. Rapid Commun. 41 (7) (2020) 1–7, https://doi.org/10.1002/marc.201900653.
[34] Q. Wang, J.B. Schlenoff, The polyelectrolyte complex/coacervate continuum, Macromolecules 47 (2014) 3108, https://doi.org/10.1021/ma500500q.
[35] C.E. Sing, Development of the modern theory of polymeric complex coacervation, Adv. Colloid Interface Sci. 239 (2017) 2–16, https://doi.org/10.1016/j.cis.2016.04.004.
[36] A.E. Neitzel, Y.N. Fang, B. Yu, A.M. Rumyantsev, J.J. De Pablo, M.V. Tirrell, Polyelectrolyte complex coacervation across a broad range of charge densities, Macromolecules 54 (14) (2021) 6878–6890, https://doi.org/10.1021/acs.macromol.1c00703.
[37] J.B. Schlenoff, Site-specific perspective on interactions in polyelectrolyte complexes: Toward quantitative understanding, J. Chem. Phys. 149 (16) (2018), https://doi.org/10.1063/1.5035567.
[38] Z.A. Digby, M. Yang, S. Lteif, J.B. Schlenoff, Salt resistance as a measure of the strength of polyelectrolyte complexation, Macromolecules (2022), https://doi.org/10.1021/acs.macromol.1c02151.
[39] W. Kunz, Specific ion effects in colloidal and biological systems, Curr. Opin. Colloid Interface Sci. 15 (1–2) (2010) 34–39, https://doi.org/10.1016/j.cocis.2009.11.008.
[40] R.S. Rabelo, G.M. Tavares, A.S. Prata, M.D. Hubinger, Complexation of chitosan with gum arabic, sodium alginate and κ-carrageenan: Effects of PH, polymer ratio and salt concentration, Carbohydr. Polym. 223 (July) (2019) 115120, https://doi.org/10.1016/j.carbpol.2019.115120.
[41] Y. Liu, B. Momani, H.H. Winter, S.L. Perry. Rheological Characterization of Liquid-to-Solid Transitions in Bulk Polyelectrolyte Complexes. *Soft Matter* **2017**, *13* (40), 7332–7340. https://doi.org/10.103a/c7sm01285c.
[42] S.L. Perry, L. Leon, K.Q. Hoffmann, M.J. Kade, D. Priftis, K.A. Black, D. Wong, R. A. Klein, C.F. Pierce, K.O. Margossian, J.K. Whitmer, J. Qin, J.J. De Pablo, M. Tirrell, Chirality-selected phase behaviour in ionic polypeptide complexes, Nat. Commun. (2015) 6, https://doi.org/10.1038/ncomms7052.
[43] C.E. Sing, S.L. Perry, Recent progress in the science of complex coacervation, Soft Matter 16 (12) (2020) 2885–2914, https://doi.org/10.1039/d0sm00001a.
[44] S. Manoj Lalwani, C. Eneh, J. Lutkenhaus, Emerging trends in the dynamics of polyelectrolyte complexes, PCCP (2020) 24157–24177, https://doi.org/10.1039/d0cp03696j.
[45] M. Rubinstein, R.H. Colby. *Polymr Physics*; Oxford, 2003.
[46] A.B. Marciel, S. Srivastava, M.V. Tirrell, Structure and rheology of polyelectrolyte complex coacervates, Soft Matter 14 (13) (2018) 2454–2464, https://doi.org/10.1039/c7sm02041d.
[47] F. Boulmedais, V. Ball, P. Schwinte, B. Frisch, P. Schaaf, J.C. Voegel, Buildup of exponentially growing multilayer polypeptide films with internal secondary structure, Langmuir 19 (2) (2003) 440–445, https://doi.org/10.1021/la0264522.
[48] R.V. Klitzing, H. Mohwald. *Proton Concentration Profile in Ultrathin Polyelectrolyte Films*; 1995; vol. 11. https://pubs.acs.org/sharingguidelines.
[49] C. Creton, M. Ciccotti, Fracture and adhesion of soft materials: A review, Rep. Prog. Phys. 79 (4) (2016) 46601, https://doi.org/10.1088/0034-4885/79/4/046601.
[50] M. Dompé, F.J. Cedano-Serrano, M. Vahdati, U. Sidoli, O. Heckert, A. Synytska, D. Hourdet, C. Creton, J. van der Gucht, T. Kodger, M. Kamperman, Tuning the interactions in multiresponsive complex coacervate-based underwater adhesives, Int. J. Mol. Sci. 21 (1) (2020), https://doi.org/10.3390/ijms21010100.
[51] D. Lee, H. Hwang, J.S. Kim, J. Park, D. Youn, D. Kim, J. Hahn, M. Seo, H. Lee, VATA: A poly(Vinyl Alcohol)- and tannic acid-based nontoxic underwater adhesive, ACS Appl. Mater. Interfaces 12 (18) (2020) 20933–20941, https://doi.org/10.1021/acsami.0c02037.
[52] M. Dompe, M. Vahdati, F. Van Ligten, F.J. Cedano-Serrano, D. Hourdet, C. Creton, M. Zanetti, P. Bracco, J. Van Der Gucht, T. Kodger, M. Kamperman. Enhancement of the adhesive properties by optimizing the water content in PNIPAM-functionalized complex coacervates. *ACS Appl. Polym. Mater.* **2020**, 1722–1730. https://doi.org/10.1021/acsapm.0c00185.